Evaluation of reservoir and cap-rock integrity for the Longyearbyen CO_2 storage pilot based on laboratory experiments and injection tests

Bahman Bohloli, Elin Skurtveit, Lars Grande, Geir Ove Titlestad, Marion H. Børresen, Øistein Johnsen & Alvar Braathen

Bohloli, B., Skurtveit, E., Grande, L., Titlestad, G.O., Børresen, M.H., Johnsen, Ø. & Braathen A.: Evaluation of reservoir and cap-rock integrity for the Longyearbyen CO_2 storage pilot based on laboratory experiments and injection tests. *Norwegian Journal of Geology,* Vol 94, pp. 171–187. Trondheim 2014, ISSN 029-196X.

Mechanical laboratory testing and interpretation of injection tests of the Longyearbyen CO2 storage pilot are used to evaluate geomechanical conditions for safe CO2 storage. The laboratory testing program includes compressive and tensile strength tests of overburden and reservoir core samples, and the injection program consists of various types of injection tests at different depths from the shallow aquifer down to the targeted sandstone reservoir. Water injection tests (leak-off, step rate and fracture tests) were analysed to determine fracture pressure for cap-rock and reservoir formations, and fracture closure pressure for some intervals. In addition, laboratory tests, well-log data and empirical correlations were used to analyse compressive and tensile strength vs. depth. Laboratory tests showed that despite the shallow depth of the reservoir, less than 700 m, the strength and stiffness of intact material is very high, and that there is significant strength anisotropy in the shale units. The high tensile strength of intact formations in combination with the presence of pre-existing fractures makes fracturing of the intact intervals very unlikely. Interpretation of the injection tests indicates that fracture pressure has a higher magnitude and gradient in the overburden than in the reservoir. In the overburden, fracture closure stress representing the minor horizontal stress is slightly lower than the vertical stress. Fracture pressure in the reservoir interval is significantly less than the vertical stress, which suggests horizontal stress to be the minimum principal stress. Therefore, opening of pre-existing vertical to subvertical fractures is considered the most likely fracturing mode in the reservoir, whereas in the overburden it is uncertain due to the marginal difference between vertical and horizontal stresses.

Bahman Bohloli, Elin Skurtveit, Lars Grande, Marion H. Børresen, Norwegian Geotechnical Institute (NGI), Sognsveien 72, 0855 Oslo, Norway. Geir Ove Titlestad, Gotic AS, Torkelstien 10, 4056 Tananger, Norway. Øistein Johnsen, Polytec, Sørhauggata 128, 5527 Haugesund, Norway Former, Norwegian Geotechnical Institute (NGI), Sognsveien 72, 0855 Oslo, Norway. Alvar Braathen, UNIS, Box 156, 9171 Longyearbyen, Norway. Present address: Department of Geosciences, University of Oslo, Postboks 1047 Blindern, 0316 Oslo, Norway.

E-mail corresponding author (Bahman Bohloli): bahman.bohloli@ngi.no

Published December 24. 2014.

Introduction

The Longyearbyen CO_2 storage pilot of Svalbard (LYB CO_2), Arctic Norway, is an onshore project targeting underground storage of carbon dioxide with the aim of reducing emissions to the atmosphere. Most drilling and seismic activity have been undertaken in the Longyearbyen CO_2 Lab well park, which is located 6 km east of the Longyearbyen community. The pilot project was initiated by the University Centre in Svalbard (UNIS) in 2007 as a feasibility for storing *c.* 64, 000 tons of CO_2 annually, emitted from the local 10 MW coal-combusting power plant (Ogata et al., 2012). So far, eight boreholes (Dhs 1–8) have been drilled targeting overburden, cap-rock and reservoir formations to gain knowledge about in situ conditions, such as physical and mechanical properties of rocks, especially the flow properties of reservoir sandstone and sealing capacity of cap-rock shale (Fig. 1).

Within a storage reservoir, density-driven fluid flow will cause CO_2 to migrate upwards. In order to prevent CO_2 to leak and reach shallow aquifers/surface, a low-permeable sealing cap rock must overlie the reservoir formation. During CO_2 injection and storage, increase in CO_2 concentration and pore pressure is expected and there are three different mechanisms that might cause CO_2 migration through the cap rock: (i) pure diffusion, (ii) seal breakage due to pressure exceeding the capillary entry pressure, and (iii) fracturing/micro-fracturing of the cap rock. The diffusion phenomenon is outside the scope of this study. The capillary sealing capacity of shale cap rock can be addressed using an experimental investigation of breakthrough pressure and flow (Hildenbrand et al., 2002; Harrington et al.,

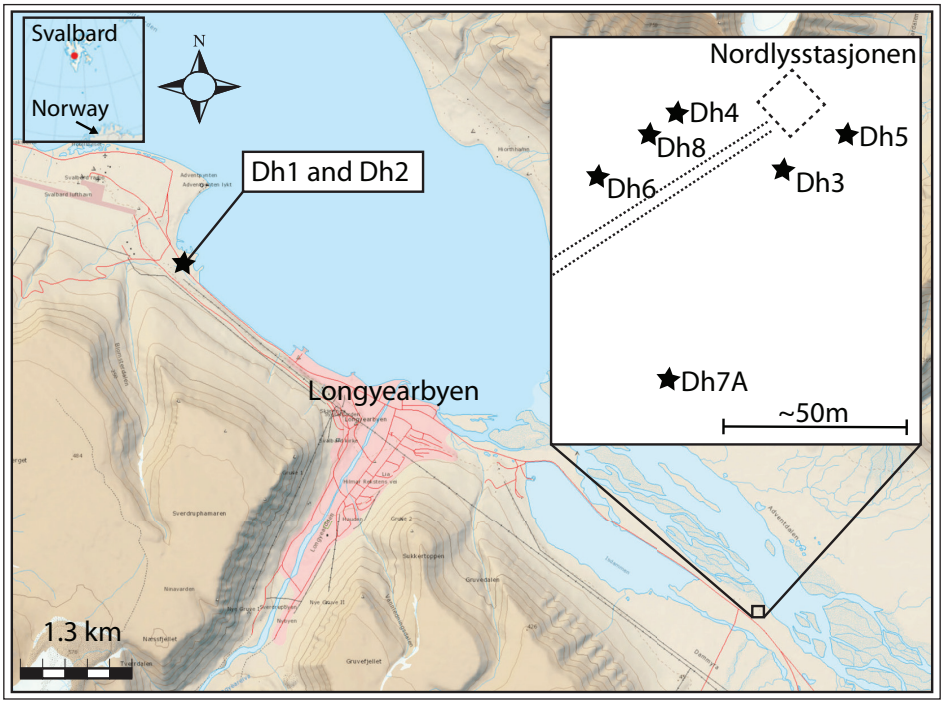

Figure 1. *Locations of the injection and monitoring wells at the Longyearbyen CO_2 site, Svalbard. (The map is by courtesy of the Norwegian Polar Institute).*

2009; Skurtveit et al., 2012). Using a similar approach as described in Skurtveit et al. (2012), the CO_2 sealing capacity for intact shale at 800 m depth in the De Geerdalen Formation, Dh2, Svalbard was found to be greater than 13.6 MPa or 136 bar (NGI, 2010).

Evaluation of cap-rock seal and risk of fracturing is an important part of the general site evaluation for CO_2 storage purposes. Fracturing is largely controlled by three parameters: (i) in situ stresses, (ii) material strength/stiffness, and (iii) the pre-existing natural fracture network. Potential seal failure due to fracturing can be addressed through coupled reservoir and geomechanical modelling of the reservoir cap-rock system (e.g., Lucier et al., 2006; Rutqvist et al., 2008). This requires knowledge of the mechanical properties and stress conditions of both reservoir and cap rock. One of the most critical aspects for ensuring safe CO_2 storage is the identification of existing faults and fractures critically oriented with respect to the stress field (Chiaramonte et al., 2013; Lee et al., 2013). This is because existing fractures and faults may have a high potential for reactivation during CO_2 injection and may provide potential migration pathways for CO_2. The tectonic history of the Svalbard area is complex and may influence the present-day orientation and magnitudes of the principal stresses. The Western Svalbard Fault Belt (WSFB), characterising the western part of Svalbard, is a transpressional fold- and thrust-belt formed under a Palaeogene contractional event (Bergh et al., 1997; Braathen et al., 1997). Based on the vitrinite data (Throndsen, 1982), the reservoir is thought to have experienced maximum burial of about 4.5 km depth during the Eocene, prior to an estimated uplift of about 3.5 km in Oligocene to latest Neogene time (Manum & Throndsen, 1978; Senger et al., 2014). This history may have affected both the magnitude and the orientation of the in situ stresses, as well as the strength and generation of natural fracture systems from compression and uplift (Ogata et al., 2012).

Within the Longyearbyen CO_2 Lab activities, core material from wells Dh2, Dh4 and Dh6 have been selected for mechanical testing. In addition, leak-off and injection tests have been performed in Dh4, Dh6 and Dh7A. In the current work, we use data from the injection tests to estimate fracture pressure and minimum in situ stress for the selected intervals of the reservoir and overburden. Detailed analysis of water injection tests together with the mechanical characterization of both reservoir and cap-rock units are combined in order to give a geomechanical assessment of the site. The results are discussed in the context of the available in situ stress data, and a simplified analytical evaluation is provided for fracturing mechanisms adjacent to the wellbores.

Stratigraphy and studied formations

The general stratigraphy of the Longyearbyen CO_2 pilot site (Fig. 2) has been described by several authors (e.g., Braathen et al., 2012; Ogata et al., 2012). Generally, the drilled formations comprise siliciclastic deposits, all showing extensive diagenetic effects including quartz overgrowth (Mørk, 2013) consistent with a burial of about 3 to 4 km before unroofing (Senger et al., 2014). From the surface downwards, they include the Cretaceous,

deltaic to marine Carolinefjellet Formation down to *c.* 150 m depth, followed by the 50 m-thick fluvial to coastal Helvetiafjellet Formation. The next units are the Jurassic marine mudstone-dominated Rurikfjellet and the organic-rich shale of the Agardhfjellet formations, underlain by the Upper Triassic–Lower Jurassic reservoir sandstones at 670 m (Braathen et al., 2012). Below this, the Knorringfjellet Formation of the Wilhelmøya Subgroup (670–701 m) comprises a condensed succession of mainly marine sandstones with mudstone interlayers. The base and top of this unit are represented by regionally recognised conglomerates, of which the latter locally show little cementation (Magnabosco et al., 2014). From 701 m to more than 970 m (in Dh4), the De Geerdalen Formation of the Kapp Toscana Group makes up a heterolithic succession, which shows a general upward coarsening. Typical deposits are the shallow-marine to coastal sandstones including tidal deltas and spits, interlayered with lagunal and marine mudstones and shales. The Net sandstone is around 30% (Ogata et al., 2012). The permafrost layer (temperature below zero degrees Celsius) in the well park extends downward to at least 120 m depth, but shallows towards the sea and finally terminates at the coast line (Christiansen et al., 2010). In a regional sense, this permafrost layer has a positive impact on the sealing capacity since most fractures and conduits are filled with ice, resulting in a significant reduction of hydraulic conductivity.

Mechanical characterisation

Laboratory testing

Mechanical characterisation of the Longyearbyen CO_2 pilot site is based on the laboratory unconfined compression and Brazil strength tests. The unconfined compression test measures the compressive strength of a cylindrical rock plug under uniaxial loading conditions. The brazil test measures the uniaxial tensile strength of the rock indirectly. A disc-shaped specimen is placed between two steel jaws so as to contact the jaws over an arc. A compressional load is applied by the jaws. This creates a tensile field inside the disc so that specimen fails in tension. The justification for this test is based on the experimental fact that most rocks in biaxial stress fields fail in tension at their uniaxial tensile strength when one principal stress is tensile and the other finite principal stress is compressive with a magnitude not exceeding three times that of the tensile principal stress (ISRM, 2007). The tensile strength of the specimen (σ_t) is calculated by Equation 1 (ISRM, 2007):

$$\sigma_t = 0.636\, P/D_t \qquad \text{Eq. (1)}$$

where P is the load at failure (in Newton), D is the diameter of the test specimen (mm), and t is the thickness of the test specimen measured at the centre (mm).

Rock cores sampled from boreholes Dh2, Dh4 and Dh6 were selected for mechanical strength testing. The laboratory program consisted of 16 unconfined compressive strength tests (UCS) and 29 tensile strength tests performed on vertically drilled specimens according to standard procedures from ASTM and ISRM (ISRM, 2007; ASTM, 2010). Test plugs were taken from the interval of 400 to 800 m depth of cores from drillhole Dh4 and from two intervals in wells Dh2 and Dh6 (Fig. 2), representing different lithologies: shale, sandstone and fault-zone material. An overview of all tests, measured strength and deformation modulus, E, is given in Table 1. Most cores, except Dh6, have been stored for more than one year and are tested in almost dry conditions. Due to the low initial water content of fresh core samples, the water content may not have a significant impact on the

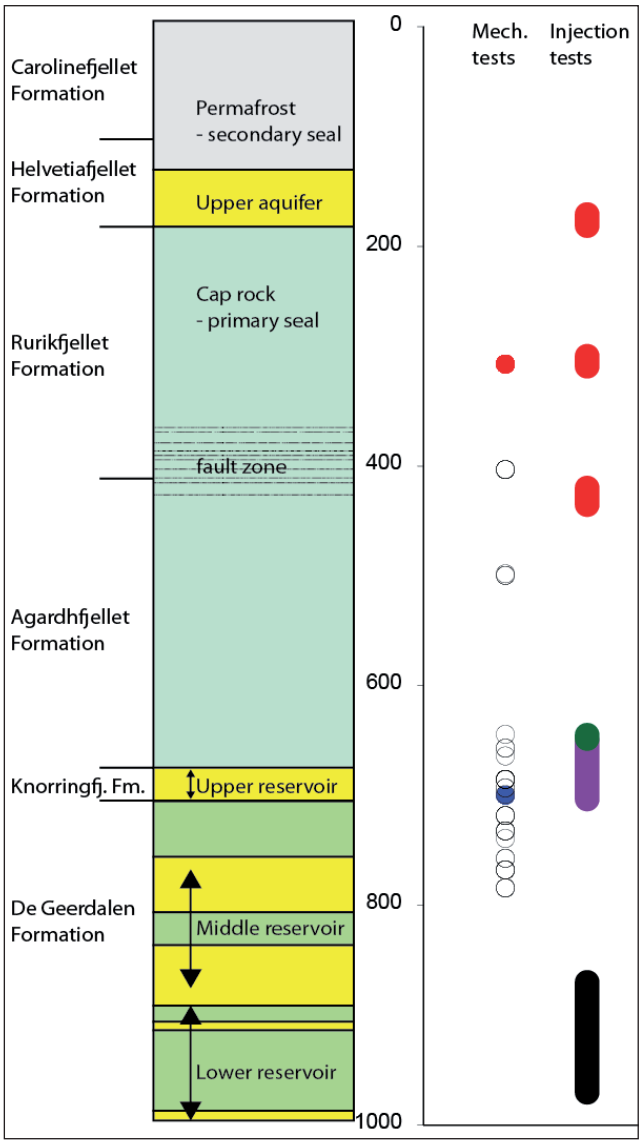

Figure 2. *Overview of the stratigraphic succession with the reservoir zones based on Dh4 (Braathen et al., 2012), and the depth interval for mechanical testing and leak-off/water injection tests used in this study. The colour code to the right shows the tests in different boreholes; red for Dh6, black/open circle for Dh4, blue for Dh2, green for Dh5R and purple for Dh7A.*

Table 1. *Mechanical characterisation and testing of plugs from boreholes Dh2, Dh4 and Dh6 (values are expressed in MPa/GPa; 1 MPa = 10 bar, 1 GPa = 10 000 bar). * parallel with bedding, ** sandstone.*

Sample No.	Well	Core depth (m)	Density (g cm^{-3})	Tensile strength (MPa)	Unconfined compressive strength, UCS (MPa)	Deformation modulus (GPa)	Formation
121	Dh6	307.00–307.13	2.62	6.86	-	-	Rurikfjellet
122	Dh6	307.00–307.13	2.62	7.28	-	-	Rurikfjellet
123	Dh6	307.00–307.13	2.61	6.34	-	-	Rurikfjellet
124	Dh6	307.00–307.13	2.61	7.76	-	-	Rurikfjellet
125	Dh6	307.00–307.13	2.59	5.53	-	-	Rurikfjellet
166*	Dh6	307.13–307.26	2.62	3.79	-	-	Rurikfjellet
167*	Dh6	307.13–307.26	2.62	3.99	-	-	Rurikfjellet
168*	Dh6	307.13–307.26	2.61	2.85	-	-	Rurikfjellet
169*	Dh6	307.13–307.26	2.61	4.63	-	-	Rurikfjellet
170*	Dh6	307.13–307.26	2.59	5.11	-	-	Rurikfjellet
171*	Dh6	307.13–307.26	2.59	3.93	-	-	Rurikfjellet
1A	Dh4	403.17	3.04	10.94	83.5	37.5	Rurikfj., Fault zone
1B	Dh4	403.17	3.04	10.73	-	-	Rurikfj., Fault zone
1C	Dh4	403.17	3.18	11.44	-	-	Rurikfj., Fault zone
1D	Dh4	403.17	3.04	10.55	-	-	Rurikfj., Fault zone
7	Dh4	498.00	-	-	70.2	8.3	Agardhfjellet Fault zone
8A	Dh4	499.46	2.60	9.39	71.5	10.3	Agardhfjellet
8B	Dh4	499.46	2.61	10.10	60.6	10.4	Agardhfjellet
9	Dh4	644.20	-	-	37.8	10.7	Agardhfjellet
12A	Dh4	656.75	2.58	10.11	76.0	9.7	Agardhfjellet
12B	Dh4	656.75	2.59	9.88	76.5	10.2	Agardhfjellet
13	Dh4	663.87	2.50	2.50	-	-	Agardhfjellet
A-1*	Dh4	685.22	2.65	2.80	-	-	Knorringfjellet
A-2*	Dh4	685.22	2.58	2.44	-	-	Knorringfjellet
B-1*	Dh4	685.22	2.58	6.65	-	-	Knorringfjellet
B-2*	Dh4	685.22	2.63	3.08	-	-	Knorringfjellet
C-1	Dh4	685.22	2.64	8.78	-	-	Knorringfjellet
C-2	Dh4	685.22	2.64	4.76	-	-	Knorringfjellet
E1	Dh2	699.62	2.39	6.27	-	-	Agardhfjellet
E2	Dh2	699.62	2.56	6.19	-	-	Agardhfjellet
D1	Dh2*	699.62	2.57	2.94	-	-	Agardhfjellet
D2	Dh2*	699.62	2.28	5.06	-	-	Agardhfjellet
16A	Dh4	693.00	-	-	120.5	18.3	Knorringfjellet
16B	Dh4	693.00	-	-	107.2	23.0	Knorringfjellet
17	Dh4	699.00	-	-	74.9	11.3	Knorringfjellet
19A	Dh4	718.14	2.41	4.75	-	-	Knorringfjellet
19B	Dh4	718.14	2.41	4.14	-	-	Knorringfjellet
19C	Dh4	718.14	2.41	6.44	-	-	Knorringfjellet
19D	Dh4	718.14	2.43	7.67	-	-	Knorringfjellet
20A	Dh4	732.08	2.65	11.52	-	-	De Geerdalen, shale
20B	Dh4	732.08	2.70	8.11	-	-	De Geerdalen, shale
20C	Dh4	732.08	2.66	10.76	-	-	De Geerdalen, shale
20D	Dh4	732.08	2.65	11.44	-	-	De Geerdalen, shale
21	Dh4	739.00	-	-	105.1	13.3	De Geerdalen, shale
22A	Dh4	757.00	-	-	125.2	16.7	De Geerdalen, shale
22B	Dh4	757.00	-	-	109.7	26.8	De Geerdalen, shale
23	Dh4	767.58	-	-	135.1	26.8	De Geerdalen, sst**
23A	Dh4	767.58	2.51	11.63	-	-	De Geerdalen, sst
23B	Dh4	767.58	2.52	10.94	-	-	De Geerdalen, sst
23C	Dh4	767.58	2.52	11.55	-	-	De Geerdalen, sst
24A	Dh4	784.00	2.49	9.84	140.0	23.3	De Geerdalen, sst
24B	Dh4	784.00	2.50	10.00	142.6	38.0	De Geerdalen, sst
24C	Dh4	784.00	2.51	10.81	-	-	De Geerdalen, sst

measured strength, but this has not been proved through reference testing of saturated vs. dry samples. This is an uncertainty and might be a source of error. Triaxial testing of rock cores may also provide more accurate strength values than the uniaxial compression strength data presented in Table 1. A detailed mineralogical study of the cap rock was performed for samples from Dh4 at 499.46 m and 656.75 m depth. Both samples show a similar mineralogy. The XRD analyses reveal that the shale contains 33–45% quartz, 35–38% illite, 12–17% albite and minor quantities of chlorite, dolomite, siderite and pyrite (totally <5%). The clay fraction by weight is about 14–18%, the silt content is rather high and the organic content (TOC) is low (NGI, 2010). The bulk density of the shale is about 2.6 g cm^{-3}, whereas that of reservoir sandstones is around 2.4–2.5 g cm^{-3}. For intact samples from the fault zone, in a décollement on top of Agardhfjellet Formation (Braathen et al., 2012), we measured a significantly higher density of 3.0 g cm^{-3} (Table 1).

The measured strength and stiffness (Table 1) varies between the different lithologies and with depth. The values of strength and stiffness are generally very high for all tested units. The tensile strength anisotropy has also been studied for the three shale lithologies using vertical and horizontal plugs, representing a fracture propagating normal to and parallel with the bedding plane, respectively. Tensile strength is lower for samples loaded parallel to bedding than those tested perpendicular to the bedding plane. Tensile strength values parallel to the bedding plane are more relevant for evaluating the initiation of horizontal fractures while those perpendicular to bedding are used for evaluation of vertical fractures. Samples from the fault zone at around 400 m depth show very high compressive and tensile strength values (Table 1), although this is an extensively deformed and fractured zone. An explanation for this might be the high density of intact samples (Table 1) possibly due to the considerable deformation and compaction within the fault zone. This particular shale represent a fault zone that is likely non-representative for the main shale layers.

Sonic log

Strength measured in the laboratory, along with the strength obtained from P-wave velocity log correlation, is plotted in Fig. 3. A site-specific correlation was made for unconfined compressive strength and tensile strength from borehole Dh4 (Table 1), and the P-wave velocity from Dh4. Note that P-wave velocity was not measured directly on the cores tested in the laboratory, therefore this correlation is based on the logged P-wave values for the corresponding depth of tested plugs assuming there is no depth shift between the log and the cores. Note that velocities in the wells are dependent on the presence of fractures, variations in fluid and effective stress in addition to the intact rock properties. Variations observed from the strength log might therefore not reflect variations only in intact rock properties. Strength correlations applied to log data is a common and useful method to extrapolate properties where physical laboratory test data are not available. A closer match between strength and log was achieved for this site-specific correlation for Longyearbyen lithologies compared to published correlations based on North Sea data (Horsrud, 2001). The velocity log for drillhole Dh4 covers the depth interval 450–800 m. To cover the shallow units, the same correlation has been used for velocity logs in drillholes Dh1 and Dh2. Although these boreholes are located at a distance of about 7 km from Dh4/Dh6 and the depths of the formations are slightly different, the major stratigraphic units are the same (Braathen et al., 2012). The correlations from logs represent an average trend and do not cover the whole range of variations obtained from the laboratory test program (Fig. 3).

Methodology for interpretation of the injection tests

Several water injection tests have been carried out in different boreholes at the Longyearbyen CO_2 pilot site to examine injectivity and fracture pressure of the formations (Fig. 2). In this study, we analysed leak-off tests (LOT), step rate tests (SRT) and fracture tests for geomechanical evaluation of the site. The pressure response during injection tests can provide valuable information on the fracture pressure and minor principal stress within the actual injection intervals. Further, the interpreted pressure response during water injection can be compared with mechanical strength data and with the vertical stress estimated from density data.

Leak-off test (LOT) and fracture tests

A plot of a typical leak-off test is presented in Fig. 4, showing injection pressure vs. time. Key observations are the leak-off pressure (LOP), formation breakdown pressure (FBP), fracture propagation pressure (FPP), instantaneous shut-in pressure (ISIP) and fracture closure pressure (FCP). Fracture pressure, also called formation breakdown pressure (FBP), is the maximum pressure obtained during injection, followed by a sudden pressure drop. In order to ensure that pressure values obtained from the LOT are reliable, a second round of pressurisation of the same interval is usually recommended. When a LOT with at least two cycles is available, the tensile strength of the formation can be determined from the difference between the formation breakdown pressure (FBP) in the first cycle and the second cycle. A separate fracture test, aiming for determination of only the fracture pressure (FBP, in Fig. 4), can be run separately from the LOT. Fracture tests may be run for a short time, on the order of minutes, or for a longer time, on the order of hours or even days. Long-time injection tests provide not only the fracture pressure of the formation but also information on

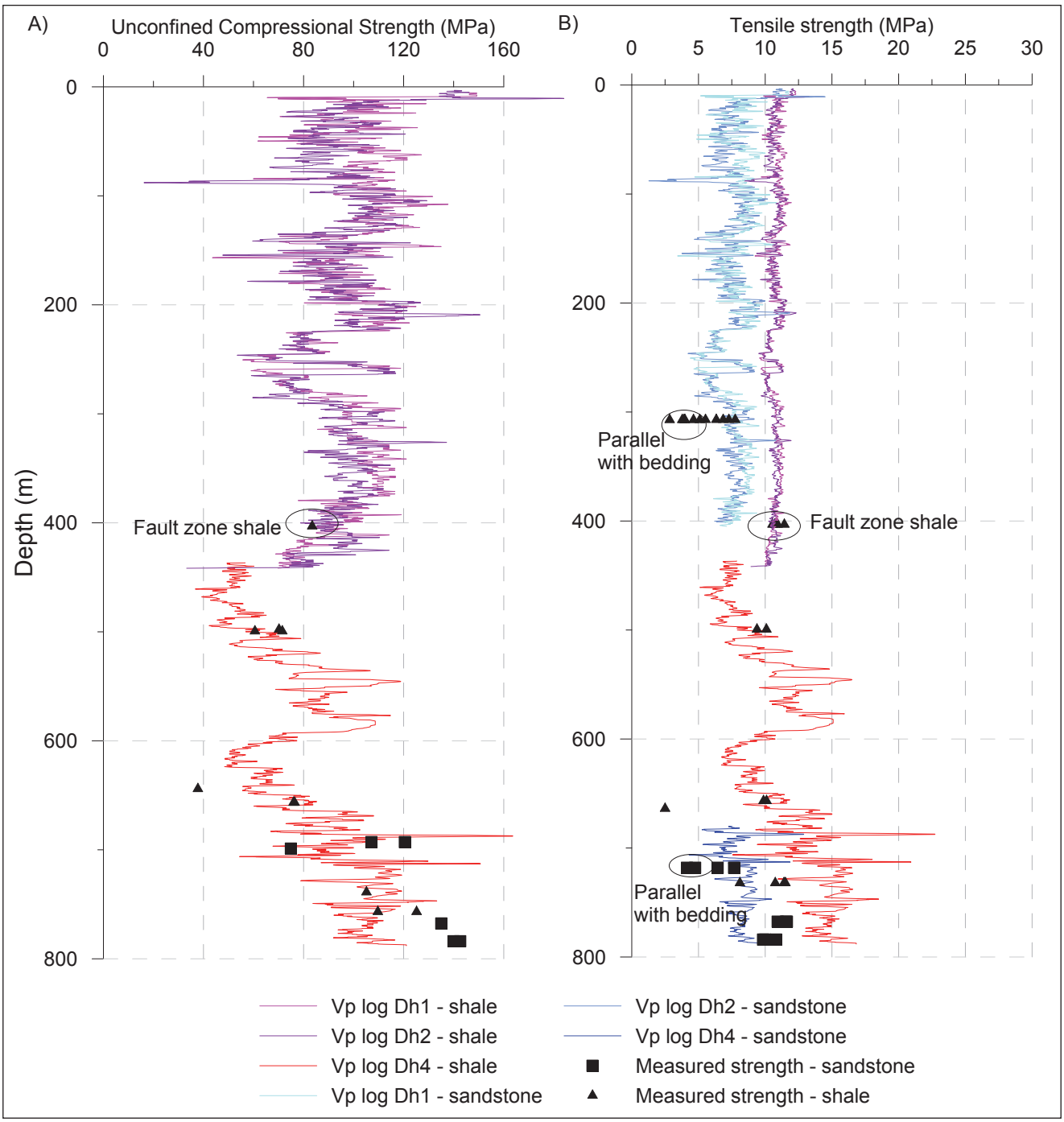

Figure 3. *Comparison of measured strength in core plugs and strength derived from velocity logs in boreholes Dh1, Dh2 and Dh4. (A) Unconfined compressive strength and (B) tensile strength.*

formation injectivity farther from the wellbore.

The magnitude of the minimum in situ stress may be indicated by LOP, ISIP or FCP, according to different interpretations (Lucier et al., 2006; Raaen et al., 2006; Zoback, 2010). Despite different opinions on the estimation of the minimum horizontal stress from the leak-off test, this is a widely used method. The minimum principal in situ stress is generally assumed to be equal to the fracture closure pressure (FCP) or the instantaneous shut-in pressure (ISIP) (Lucier et al., 2006). However, there are different recommendations on how to determine the magnitude of the minimum principal stress from leak-off and fracture tests. Raaen et al. (2006), for instance, stated that there is no general simple relation between leak-off pressure (LOP), ISIP and the minimum in situ stress. They suggested a Flowback Test for accurate determination of the minimum principal stress. On the other hand, Zoback (2010) suggested that leak-off pressure represents the minimum principal stress. Furthermore, White et al. (2002) showed, based on high-quality leak-off tests, that both FCP and ISIP

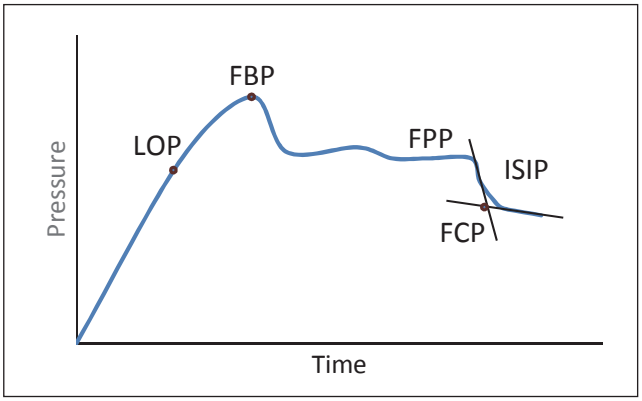

Figure 4. Schematic presentation of leak-off test and the parameters obtained from the plot of pressure vs. time (modified after Zoback, 2010). Leak-off pressure (LOP) is the pressure when the pressure-time curve deviates from linearity. The peak pressure that is followed by a sharp pressure drop is considered to be the formation breakdown pressure (FBP) or simply called fracture pressure. The fracture propagation pressure (FPP) is the stabilised pressure level which may be observed after the peak pressure. The abrupt pressure drop following pump shut-in is called the instantaneous shut-in pressure (ISIP). The fracture closure pressure (FCP) is the pressure at which the created fracture is closed off.

provide better estimates of the minimum principal stress than the LOP. In this study, we use FCP to estimate the magnitude of the minimum horizontal stress.

Step rate test (SRT)

A step rate injection test is normally used to estimate the transition from matrix (or radial) flow to fracture-dominated, more linear flow. The injection rate is increased stepwise and the corresponding pressure is measured (Fig. 5A). For every rate, injection continues until the pressure stabilises. Fracture pressure is inferred from a significant change in a plot analysing the slope of pressure vs. injection rate (Fig. 5B).

Fracture pressure of overburden and reservoir formations

Several injection and fracture tests have been conducted in the different boreholes to examine the injectivity of the Knorringfjellet and De Geerdalen formation sandstones and to determine the maximum pressure that sealing formations can sustain prior to fracturing. These include the Step Rate Test (SRT), Leak-Off Test (LOT) and fracture tests. Targets of drillhole Dh6 were the overburden units, while the testing intervals for boreholes Dh4 and Dh7A were the Knorringfjellet and De Geerdalen formations (Fig. 2). The types of tests utilised for this study are given in Table 2.

Step rate test and fracture test at 171–181 m depth, Dh6 (Festningen sandstone of the Helvetiafjellet Formation)

The uppermost test section is the 171 to 181 m depth interval of borehole Dh6. This section has been tested for fracturing and injectivity examination (Table 2). The fracture pressure of the formation was achieved in a step rate test (SRT), as plotted in Fig. 6A. The SRT was carried out with different injection rates of 30, 50, 80, 140 and 200 l min^{-1}. A fracture test was also performed in this interval (Fig. 6B).

The fracture test has been conducted with an injection rate of 1000 l min^{-1}. The pressure fluctuation observed in the graph (Fig. 6B) is due to a vibration of the pump line at a high injection rate (Titlestad, 2011), which makes the pressure record somewhat noisy and unclear. However, the trend of average pressure throughout the test (plotted with a dashed black line) shows signs of fracturing in the form of pressure drops that are observed during the constant injection rate.

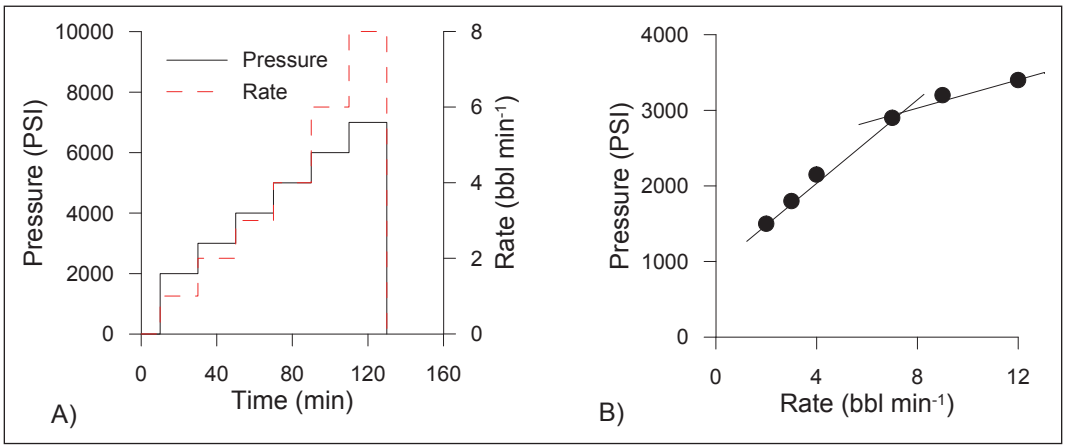

Figure 5. (A) Typical step rate injection test. The injection rate is increased stepwise but is constant during each step. (B) The corresponding pressure is recorded and analysed to determine whether or not fracturing has occurred. The intersection between the two adjoining linear curves is interpreted as the fracture pressure

Table 2. *Overview of injection and fracture tests utilised to estimate the minimum in situ stress and fracture pressure profile at the Longyearbyen CO_2 storage site.*

Section	Testing depth (m)/ Formation	Number and type of tests	Well No.
Overburden	171–181 Helvetia Fm.	Step rate test (SRT) Fracture test	Dh6
	300–309 Rurikfjellet Fm.	2 leak-off tests (LOT)	
	420–435 Agardhfjellet Fm.	2 leak-off tests (LOT)	
Reservoir	650–703 Lower Agardhfjellet Fm. Upper Knorringfjellet Fm.	2 step rate tests	Dh7A
	870–970 De Geerdalen Fm.	Step rate test	Dh4

In order to determine the fracture pressure of the Helvetia formation, data of the step rate test are presented in a plot of pressure vs. injection rate (Fig. 7A). Note that pressure data in Fig. 7 have been converted to bottom hole by adding a static water column of 176 m (middle of the injection section) to the surface pressure. Two trend lines can be fitted to the data, and from their intersection the fracture pressure is estimated for the tested section. Thus, a fracture pressure of 42 bar is obtained for this interval (Fig. 7A), though the accuracy suffers from having few data points beyond the fracture opening pressure to confidently assign a precise linear curve fit. In order to improve the accuracy of the fracture pressure value, we combined data from the fracture test with those of the step rate test. In Fig. 7B, data of the fracture test (the far right point) fit well within the second linear trend of data which represents the fracturing regime. Intersection between the two trend lines indicates 43 bar as the fracture pressure at 171–181 m. This plot shows a fracture pressure for the interval 171–181 m depth at around 42–43 bar.

Leak-off tests at 300–309 m depth, Dh6 (Rurikfjellet Formation)

Two LOTs have been carried towards a 9 m open hole in the 300–309 m interval of drillhole Dh6, targeting the Rurikfjellet Formation mudstones. A plot of the test results shows the signatures of fracturing or opening of pre-existing fractures during the first test (Fig. 8), with a typical pressure behaviour in the beginning followed by a sharp pressure drop ascribed to fracture propagation in the later stages. LOT 2 (Fig. 8) shows reopening of the already created fracture that is suggested by a smaller pressure drop in the initial state than that of the first test. The first leak-off test gives a fracture pressure of about 55 bars for 300–309 m depth. This pressure was read at the

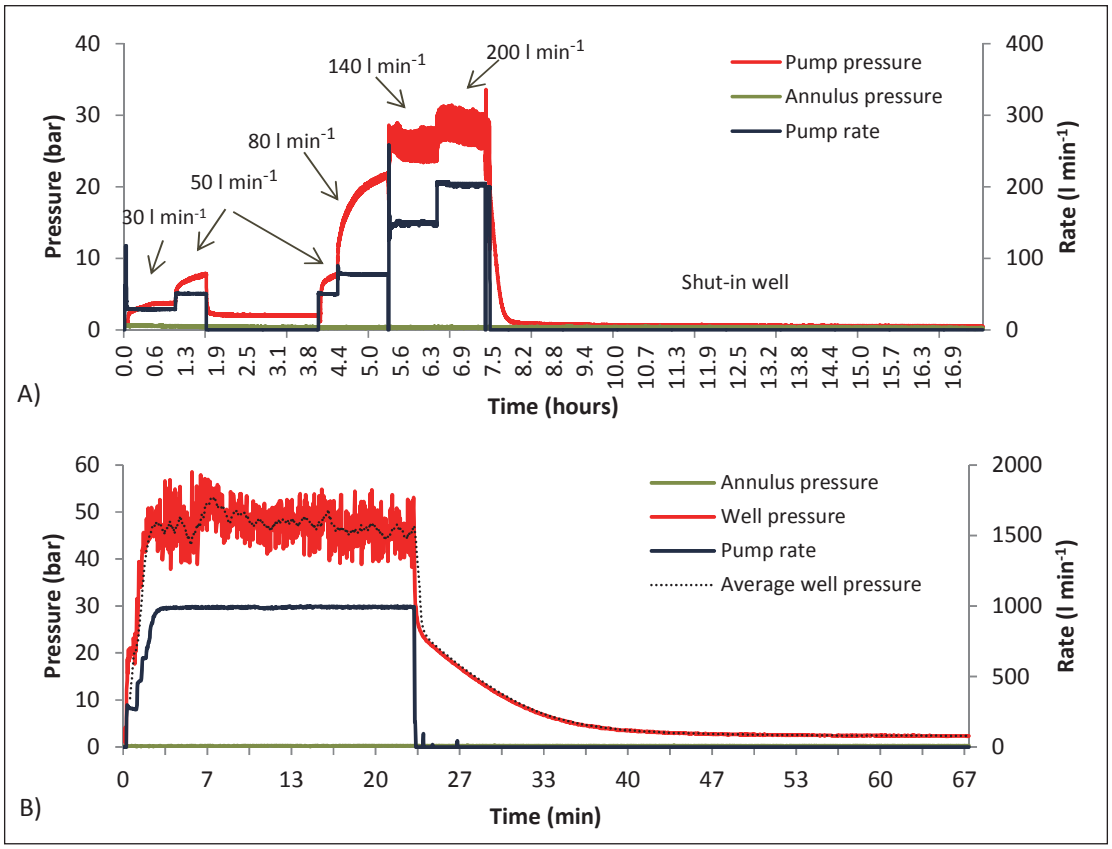

Figure 6. *Step rate test (A) and fracture test (B) at 171–181 m depth, borehole Dh6 (modified from Titlestad, 2010). The tests target the Festningen sandstone of the Helvetiafjellet Formation. Pressure values in both figures represent the pump pressure recorded at the surface.*

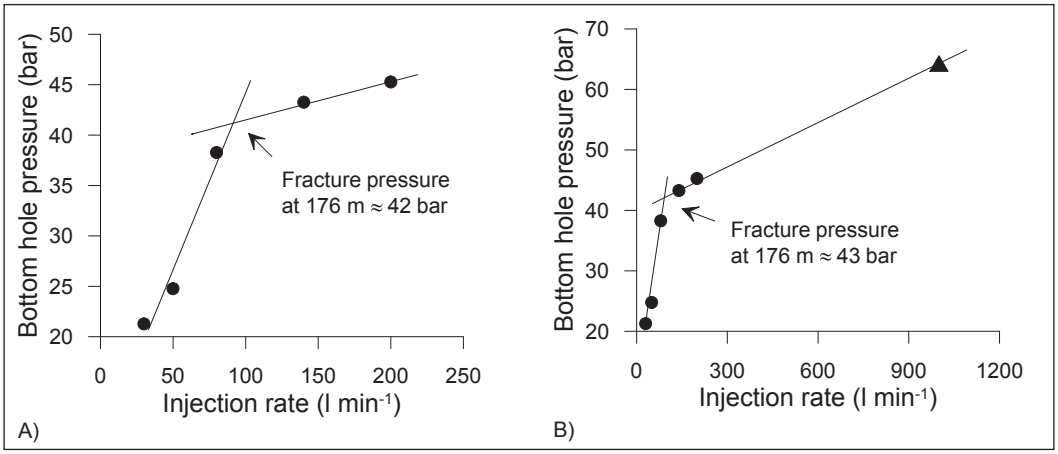

Figure 7. Determination of the fracture pressure from the step rate test (SRT) in the 171–181 m depth interval of borehole Dh6. (A) Bottom hole pressure from the step rate test. (B) Integrated data of SRT and the fracture test (triangle). The bottom hole fracture pressure is about 42–43 bar.

surface pump and is converted into bottom hole pressure by adding the static pressure of the water column and assuming that fracturing occurred in the middle of the open section, i.e., at 304.5 m. The viscous friction pressure loss in the injection line was about 2 bars (Fig. 8), which should be subtracted from the readings. Thus, the bottom-hole pressure (P_{frBH}) will be (Titlestad, 2011):

$$P_{frBH} = P_{frS} + P_{hyd} - P_{fric} \quad \text{Eq. (2)}$$

where P_{frS} is the fracture pressure recorded at the surface, P_{hyd} is the hydraulic pressure of the water column (30.45 bar at 304.5 m depth) and P_{fric} is the friction pressure loss of 2 bars in the injection line, estimated from Fig. 8. The bottom hole fracture pressure calculated from Eq. (2) is thus: P_{frBH} = 83.45 bars.

The fracture closure pressure (minimum in situ stress) can be estimated from the pressure curve in the LOT 2 (Fig. 8) and gives a fracture closure pressure of about 33 bar at the surface, equal to 63.5 bars bottom hole pressure in the middle of the injection zone. The two LOTs allow us to estimate the tensile strength of the formation. Tensile strength is the difference between the fracture pressure and the reopening pressure. Since the testing conditions are the same for both fracturing cycles, the difference between the first pressure peak (55 bar) and the second one (44 bar) gives an estimation of the tensile strength of the formation. The tensile strength of the formation is, thus, 11 bars which is low compared to the tensile strength of intact shale samples from Dh6 measured in the laboratory (Table 1). An explanation for this observation is that the leak-off test shows the tensile strength of pre-existing fractures at wellbore scale whereas the laboratory tests measure the tensile strength of intact core specimens at a much smaller scale.

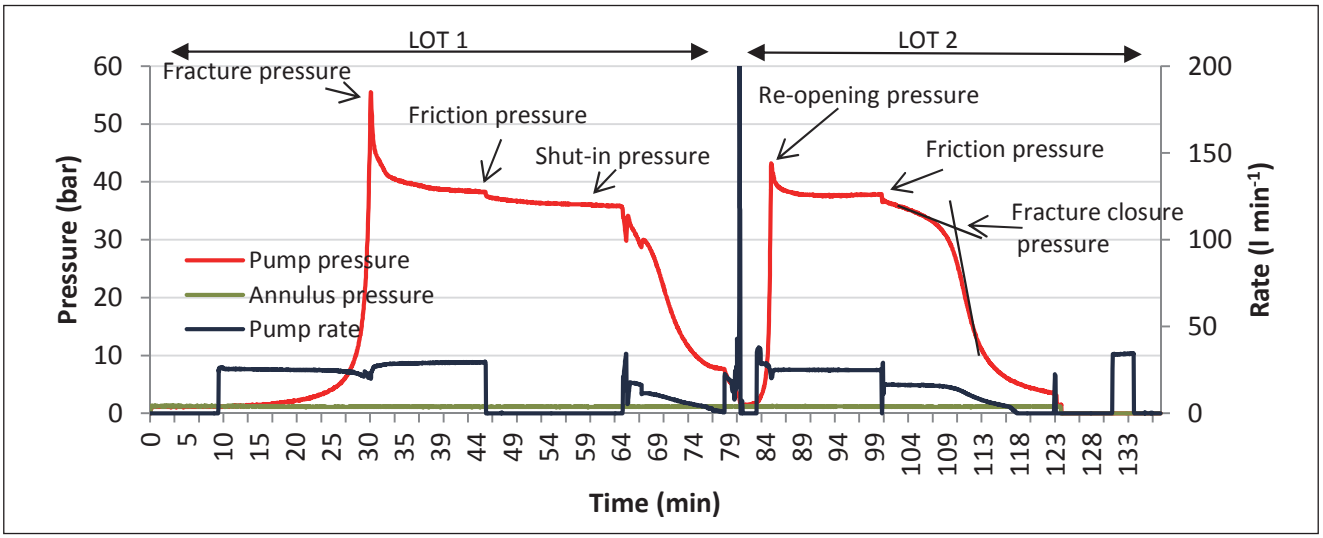

Figure 8. Plot of the two leak-off tests at 300–309 m depth (borehole Dh6) showing pressure recorded at the surface vs. time (modified from Titlestad, 2011). The peak pressure of 55 bars (red curve in the left plot) indicates the fracture pressure. The second test (right) shows a lower peak pressure corresponding to a reopening of the fracture created during the first test.

Leak-off tests at 420–435 m depth, Dh6 (upper Agardhfjellet Formation)

Two LOTs have been carried out at 420–435 m depth in Dh6 (Fig. 9), targeting the upper shale units of the Agardhfjellet Formation. As for some of the other tests, pressure is recorded at the surface pump. LOT 1 show a peak pressure of 75 bar, where fracturing of the rock or reopening of natural fractures probably occurred. LOT 2 also shows signatures of reopening at a similar pressure of about 75 bars. In accordance with the water-column considerations presented above, a recalculation of the surface pressure data to the middle of the tested interval (427.5 m) suggests a fracture pressure of about 118 bar. This value neglects the friction pressure loss in the liner; however, a friction pressure loss of 2 bars has been recorded for the depth interval 300–309 m (Fig. 8). A simple extrapolation (as both boreholes have the same diameter) will lead to a friction pressure loss of about 3 bars for a test interval of 420–435 m depth. Thus, the bottom hole fracture pressure will be about 115 bar.

The fracture closure pressure or minimum principal stress can be estimated from the declining pressure curve of the LOTs. The first LOT gives a fracture closure stress of about 65 bar while the second LOT suggests about 55 bar of surface pressure. Considering a 42.7 bar hydraulic pressure and 3 bar friction pressure drop for the injection line, the fracture closure stress will be in the range 94–104 bar for the depth of 427 m.

Step rate tests at 650/670–703 m depth, Dh7A (Knorringfjellet Formation and lower Agardhfjellet Formation)

Two step rate tests (SRT) have been conducted in well Dh7A at the depth interval 650–703 m, targeting the Knorringfjellet Formation. Test SRT 1 comprised seven different steps with injection rates ranging from 30 to 250 l min^{-1}. The second, SRT 2, was repeated in the same interval but the number of steps was increased to ten and the injection rate raised up to 1000 l min^{-1}.

In order to determine fracture pressure from the SRTs, the injection pressure was plotted against injection rate (Fig. 10). The plotted pressure values represent the bottom hole pressure (BHP). The BHP was calculated by

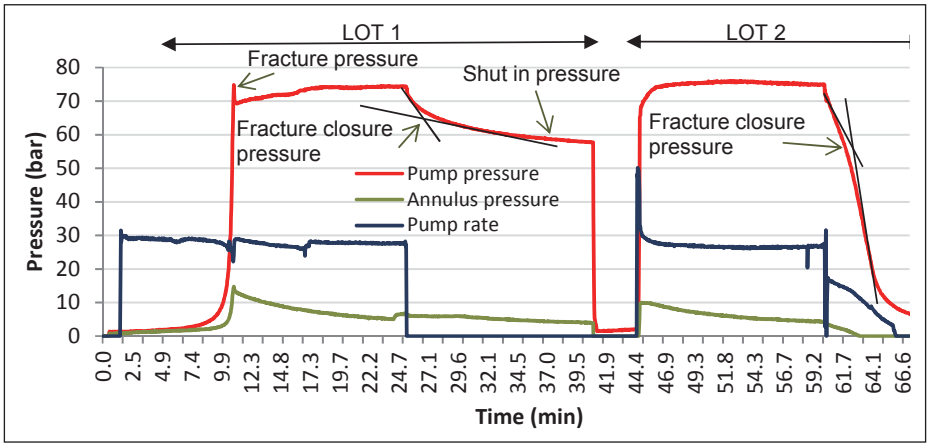

Figure 9. Leak-off tests in the depth interval 420–435 m, borehole Dh6 (modified from Titlestad, 2011). The formation has most likely been fractured at 75 bar pump pressure (peak pressure), which is equivalent to 115 bar bottom hole pressure.

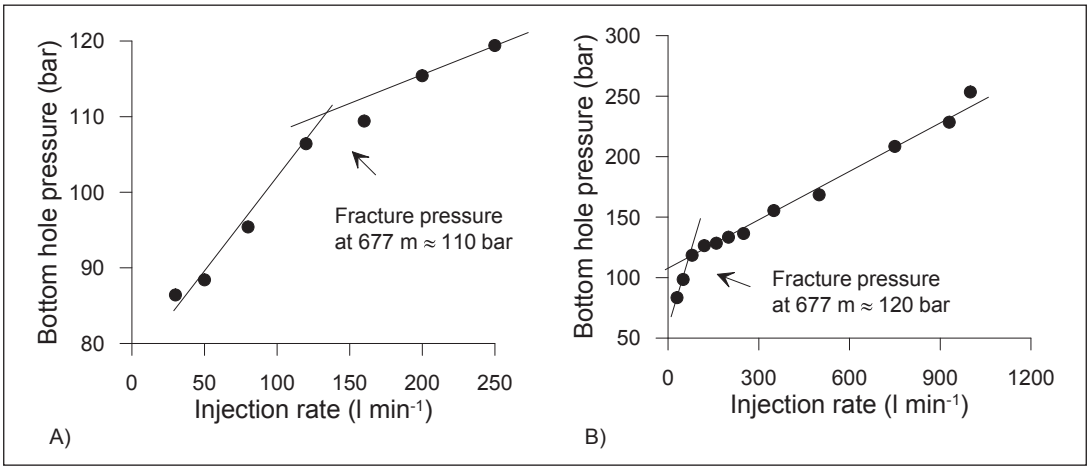

Figure 10. Fracture pressure from two step rate tests at a depth of 650–703 m, borehole Dh7A. (A) SRT 1 suggests a fracture pressure of about 110 bar, and (B) SRT 2 indicates a fracture pressure of 120 bar.

adding the hydraulic pressure of the 677 m water column to the values recorded at the surface. Friction pressure loss is neglected for calculation of the bottom hole pressure here, since no data are available.

SRT 1 (Fig. 10A) shows a change in the slope of the pressure-rate curve after the fourth step. The steep trend most likely indicates injection into the rock matrix, whereas the second trend line shows a lower slope for the pressure curve and thus indicates fracture injection. The intersection between these two trend lines indicates the fracture pressure of the formation which is about 110 bar. SRT 2 (Fig. 10B) shows a clear change in the slope of the pressure curve and thus a significantly increased injectivity after the third step. This confirms that either pre-existing fractures are opened or new fractures are created at a pressure of about 120 bars. Thus, the average fracture pressure at a depth of 677 m (the middle of the interval 650–703 m) is around 110–120 bar based on the interpretation of the two SRTs.

Step rate test at 870–970 m depth, Dh4 (lower De Geerdalen Formation)

The SRT presented here is one of the five injection tests carried out in the depth interval 870–970 m of borehole Dh4, targeting the lower part of the De Geerdalen Formation. At this level, the succession consists of interlayered sandstones and shales, and includes several 0.5 to 2 m-thick dolerite sills (Senger et al., 2014). The pressure during the step rate test was measured using a down-hole memory sensor installed at 855 m depth while the injection rate was measured at the surface (Titlestad, 2010). Therefore, the data presented here show the pressure at a depth of 855 m. For converting pressure to the values at the middle of the injection interval, a hydraulic pressure of 65 m of water column (855 to 920 m), is added to the recorded pressures.

The step rate test included eight steps of injection, each step lasting for 10 minutes. The bottom hole pressure vs. injection rate of the SRT is used to determine the fracture pressure (Fig. 11). It shows a linear behaviour in the beginning but deviates from the initial linear trend after the 5th step. Two trend lines can be fitted to the data, the intersection of which indicates transition from matrix- to fracture-injection. When converted to bottom hole pressure in the middle of the open section at 920 m, a fracture pressure of 130 bar is obtained.

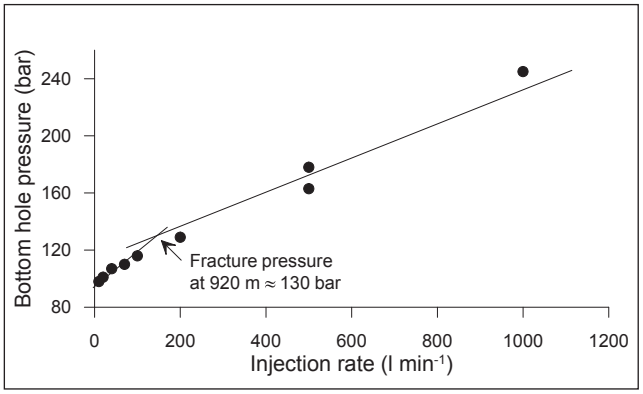

Figure 11. *Step rate test in borehole Dh4 in the depth interval 870–970 m. Intersection between the two trend lines indicates a reopening of existing fractures or fracturing of the reservoir formation in the middle of the injection interval at around 130 bar pressure.*

Summary and discussion

Evaluation of the cap-rock seal and the risk of fracturing is an important component in the assessment of CO_2 storage sites as discussed, for instance, in Rutqvist et al. (2008). In this study, we determine fracture pressure and analyse the fracturing of different formations based on the injection tests carried out at various depths and in different boreholes. The fracture pressure values are then compared with the in situ stress and tensile strength data to explain the type of fracturing during injection tests and the possible influence of pre-existing natural fractures. A summary of the estimated vertical stress (lithostatic gradient), minimum in situ stress interpreted from fracture closure pressure, fracture pressure and tensile strength for the tested intervals is given in Table 3. For intervals where injection tests and mechanical testing do not directly overlap, a best estimate for tensile strength is based on an evaluation of nearby data and correlation logs (Fig. 3).

Fracture pressure

The interpreted fracture pressures and minimum in situ stress (from closure pressure) summarised in Table 3 are presented together with the lithostatic gradient for comparison in Fig. 12. Uncertainties related to the data and interpretation of the possible fracture opening mode will be discussed in detail in the following sections.

The interpreted fracture pressure is defined as the pressure that is able to fracture a formation and cause fluid loss from the wellbore into the induced fracture. Several factors, including relative magnitude of in situ principal stresses, tensile strength of the rock mass, well orientation, and the presence and nature of pre-existing fractures influence the measured fracture pressure. Fracture pressure (P_{frac}) for vertical fractures in a vertical wellbore in low-permeable formations can be calculated using the equation by Zhang (2011):

$$P_{frac} = 3\sigma_{min} - \sigma_H - p - \sigma_{TH} + \sigma_t \quad \text{Eq. (3)}$$

where σmin is the minimum horizontal stress, σ_H is the maximum horizontal stress, p is reservoir pore pressure, σ_{TH} is the thermal stress and σ_t is the tensile strength of the rock.

Formation of a horizontal fracture in a vertical borehole requires a pressure exceeding the sum of the vertical stress, σ_v, and the tensile strength σ_t:

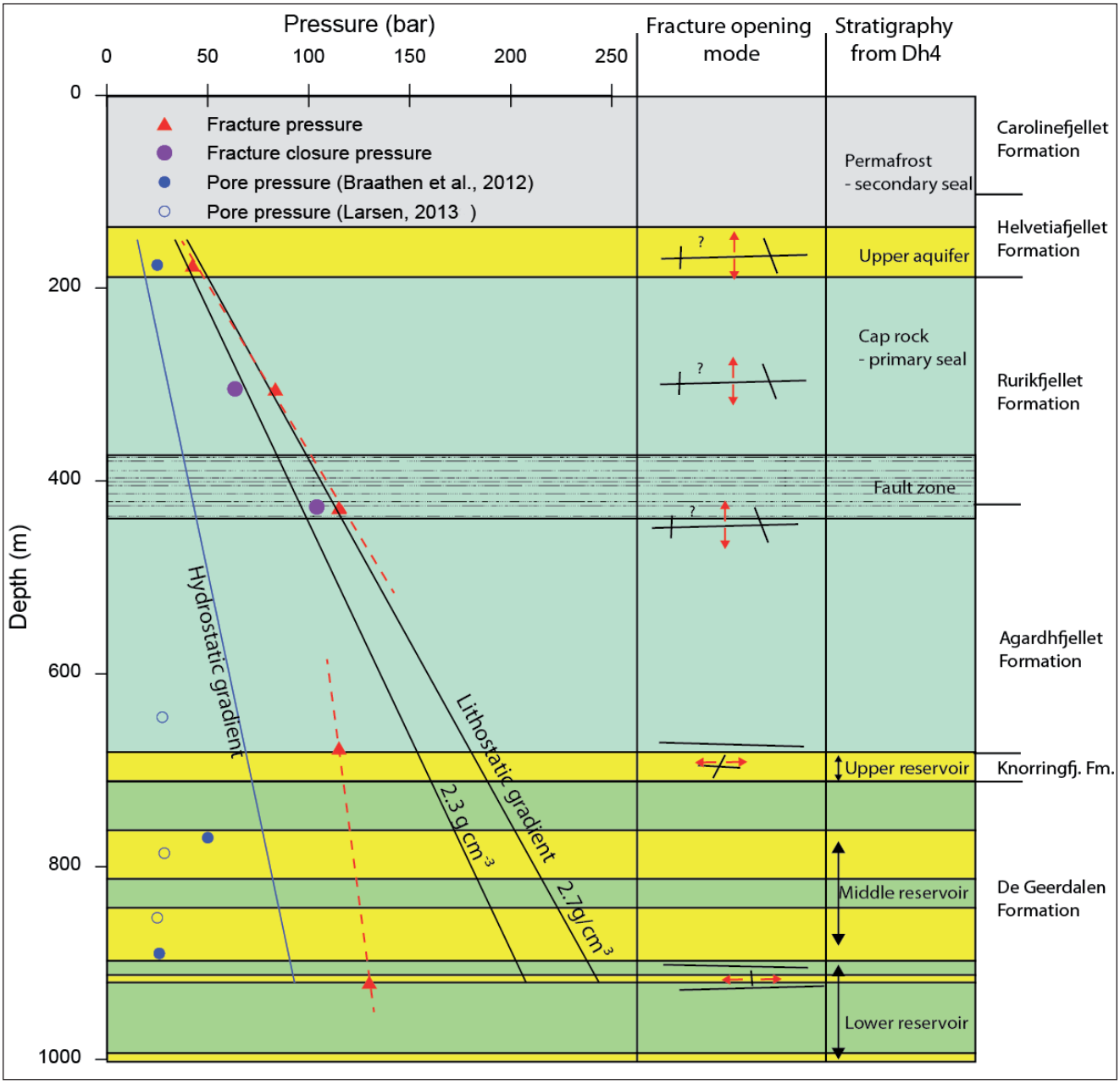

Figure 12. *The interpreted fracture pressure (red triangles), possible fracture gradients (red dashed line) and fracture closure pressure representing the minimum in situ stress (purple dots). A lithostatic gradient is added for the range of densities discussed in the paper. Measured pore pressures and a hydrostatic gradient are added for clarity. The middle column shows the possible fracture opening mode (red arrows) interpreted for critical pressure build-ups in the different formations. The stratigraphic succession in the right-hand column is based on borehole Dh4 (Braathen et al., 2012).*

$$P_{frac} = \sigma_v + \sigma_t \qquad \text{Eq. (4)}$$

The formation of horizontal vs. vertically oriented fractures depends on both the relative magnitude of in situ stresses (i.e., stress anisotropy) and the directional tensile strength of the formation (tensile strength anisotropy). However, the magnitude and orientation of the maximum horizontal stresses have not been analysed, based on the current dataset.

Tensile strength

Both tensile and compressive strength is measured in the mechanical test program and these data are further used to produce mechanical logs of the drillholes. A characteristic feature of the measured strength of the formations at the LYB CO_2 site (Table 1) is the high strength compared to the present shallow burial depth. A rather deep maximum burial depth of 3.5–4.5 km (Throndsen, 1982; Senger et al., 2014) preceding a long period of uplift may have caused significant cementation of the shale and, thus, a higher strength compared to the North Sea shale units (Horsrud, 2001) and other uplifted Barents Sea shale formations (Makurat et al.,

1992; Gabrielsen & Kløvjan, 1997). Tensile strength is an important factor controlling the fracture pressure in Eq. (3) and Eq. (4). The high tensile strength of both reservoir rock (40–120 bar) and overburden shale (40–70 bar) presented in Table 3, implies that the interpreted fracture pressure from the injection tests (Fig. 12) is related to reopening of existing fractures or layering in the formations. The tensile strength of pre-existing fractures might range from zero to a certain strength, depending on the cohesion of the fracture.

Tensile strength for both vertical and horizontal samples has been measured at different depths. The horizontal tensile strength is lower than the vertical tensile strength. This anisotropy, defined as tensile strength parallel with bedding (horizontal) divided by the tensile strength perpendicular to bedding (vertical), is found to be 0.6 and 0.64 for the Rurikfjellet and Agardhfjellet formations, respectively, whereas for the sandy Knorringfjellet Formation it is 0.55. Thus, anisotropy is highest for the Knorringfjellet Formation. The spread in measured strength is highest for horizontal tensile strength and could be related to the subhorizontal layering of the shale formations (Ogata et al., 2012).

Stress data

In Fig. 12, the measured fracture pressure in the overburden fits nicely with the upper range of the lithostatic gradient; thus, a fracture gradient (red dotted line) close to the lithostatic gradient is suggested. However, there are several uncertainties related to the parameters controlling fracture pressure for both vertical fractures, Eq. (3), and horizontal fractures, Eq. (4), that need to be evaluated.

The vertical stress (lithostatic gradient) is usually calculated from the density log, but a traditional density log is not available here; so, for this work, it was estimated from the available density data presented in Table 1. The density values show a wide range of 2.3–3.2 g cm^{-3}, with an average of 2.6 g cm^{-3}. The top 60–80 m section consists of unconsolidated sediments under permafrost (Braathen et al., 2012). The density of this zone is more uncertain and depends on the initial composition, sorting and packing of the sediments. Values in the range of 1.2–2.0 g cm^{-3} for loose packing and 2.0–2.5 g cm^{-3} for densely packed wet sediments are quite common. The density of the permafrost layer down to 120 m, covering both unconsolidated sediments and lithified rocks, will be lower due to the ice with a density of 0.92 g cm^{-3} filling the pore space. We use the density of 2.5 g cm^{-3}, which is a representative average value for the overburden units based on measurements from tested samples (Table 1), combined with a low range of 2.3 g cm^{-3} for the top 120 m to account for the less dense 60–80 m unconsolidated layer and 120 m of frozen sediment and rocks (Braathen et al., 2012). Similar gradients have been proposed by other researchers (e.g., Bælum et al., 2012). It must be noted that the vertical gradient is based on few data points and there is therefore some uncertainty associated with these values.

Pore-pressure data and hydrostatic gradient have been added in Fig. 12 to illustrate the low pore pressure measured in the reservoir compared to the hydrostatic gradient. Pore pressure has a direct impact on fracture pressure for vertical fractures, through the magnitude of horizontal stress and due to poro-elasticity (Biot, 1941; Terzaghi, 1943). A low pore pressure can result in a low horizontal stress and thus a lower fracture pressure for the opening of vertical fractures.

Due to permafrost, the pore pressure can be zero at the bottom of the permafrost layer at a depth of 120 m (Braathen et al., 2010), and will increase downwards according to the hydrostatic pressure (Fig. 12). However, the rather shallow Festningen Formation shows a slight overpressure at 170–180 m depth compared to a hydrostatic gradient starting from the surface. This might indicate a hydrostatic pore pressure starting from the surface for the overburden shale. Pore pressure, as recorded in various levels of the De Geerdalen reservoir formation and in the lower cap-rock shale, is very low (i.e., <30 bar) and is largely under-pressured compared to a hydrostatic system (Braathen et al., 2010). The reason for this enigmatic under-pressure is not clear, but is probably linked to the tectonic history and uplift.

The minor horizontal stress is usually determined from the fracture closure stress from injection tests which give a direct measure of the minimum in situ stress of the formation. Closure stress has been estimated from leak-off tests of the Rurikfjellet Formation and the Upper Agardhfjellet Formation, with values of 63.5 bar and 94 bar, respectively (Fig. 12). These values, corresponding to the minimum in situ stress, are thus slightly below the lower estimate of vertical stress (lithostatic gradient) presented in Fig. 12. Thus, the vertical stress might not be the minimum in situ stress. There are also uncertainties in the interpretation of closure stress; however, the closure pressure cannot be higher than the fracture propagation pressure (FPP) which is only a few bars higher, so the degree of uncertainty is greater towards the lower boundary. Also, a vertical stress value lower than the lower estimate given by 2.3 g cm^{-3} is less likely, albeit there are uncertainties related to densities of the overburden units as described above. Based on the present dataset, the interpreted closure stress represents a minor horizontal stress with a magnitude slightly below the vertical stress for the overburden units. A closure stress has not been determined for the two injection intervals in the reservoir (650–703 m and 870–970 m depth). Therefore, the magnitude of the minimum principal stress in the reservoir is not known. However, the low fracture pressure observed in the reservoir section might give an indication of a rather low minimum horizontal stress. In general, the magnitude of the minor horizontal stress may be

reduced due to the effect of poro-elasticity or thermally induced stresses. For the LYB CO_2 site, the low fracture pressure may be explained by (i) poro-elasticity through the observed low pore pressure (Fig. 12) and (ii) thermal stresses caused by the large difference between the temperature of injection fluid and that of the formation in the deeper reservoir units.

Geomechanical assessment

The interpreted fracture pressure is compared with the tensile strength data and lithostatic gradient to better understand the mode and orientation of induced fractures and discuss the observed change in fracture pressure gradient with depth. Within the overburden, three fracture pressures are interpreted: one from an upper aquifer and two from shale units (Table 3). The best quality injection test for fracture pressure interpretation is in the Rurikfjellet Formation (300–309 m). This test shows a classical behaviour which allows for interpretation of the fracture pressure and closure stress (minimum in situ stress). In addition, an estimate of the in situ tensile strength of the rock mass can be made, which can be directly compared to the tensile strength data of intact rock measured in the laboratory for the same interval. The in situ tensile strength, determined from the injection test based on the difference between the first and second pressure peaks in the LOT (11 bar), is quite low compared to the measured tensile strength of the intact rock which is 40 bar (range 29–51 bar) parallel with bedding and 67.5 bar (range 56–78 bar) perpendicular to bedding. The small difference of 20 bar between the fracture pressure of this formation (83 bar) and the closure pressure after shut-in (63.5 bar), combined with the low in situ tensile strength of 11 bar (from the injection test) and high tensile strength of intact rock measured for mechanical testing (Table 1) indicate that fracturing of the intact formation is not likely, neither for horizontal nor for vertical fractures. Reopening of pre-existing fractures is a more likely scenario for this interval. A back calculation of the maximum horizontal stress using Eq. (3) under the assumption of a hydrostatic pore pressure and neglecting the effect of thermal stresses indicates a slight horizontal stress anisotropy of 1.4 to explain a vertical fracture with an in situ tensile strength of 11 bar. A larger anisotropy of 2.3 would have been required in order to generate a vertical fracture in the intact rock with a tensile strength of 67.5 bar. The latter is a very high anisotropy factor and is not consistent with the in situ tensile strength of 11 bar.

For the other two intervals in the overburden, Festningen and Agardhfjellet formations, the mechanical data are not from the same interval where the leak-off tests were performed. In addition, injection tests do not have the same technical quality for interpretation as for the Rurikfjellet Formation. However, tensile strength is assumed to be high also in these intervals based on information from the correlation logs (Fig. 3), and the trends of fracture stresses for the three intervals in the overburden are consistent and comparable with the gradient of vertical stress. Fracturing of the intact formation would have required a higher fracture pressure than observed. This observation and the nice fit with the vertical stress gradient indicate that reopening of existing fractures is the dominant mechanism also in these tests.

Detailed logging of fractures in drillcores and outcrop analogs shows an abundance of low-angle (horizontal to subhorizontal) shear fractures in the massive to laminated shale interval within the upper reservoir zone (Ogata et al., 2011, 2012) and in the overburden (Elvebakk, 2010). The observed closure pressure within the overburden units indicates a minimum horizontal stress slightly lower than the vertical stress. This close correspondence with minimum horizontal stress (closure stress) and vertical stress together with the possible large presence of horizontal to subhorizontal fractures in the overburden might favour not only the opening of vertical fractures, but also horizontal to subhorizontal fractures. The actual mode will depend on the presence, orientation and filling material (cohesion) of fractures for the actual interval.

Within the reservoir section, fracture pressure is interpreted for two well tests, one in the upper reservoir and one in the lower. The two fracture pressures are significantly lower than the vertical stress range for this depth (Fig. 12). This is taken as a clear indication that the minimum principal stress is horizontal. Comparison of the tensile strength data (Table 3) and correlation logs (Fig. 3) with the fracture pressure (Fig. 12) indicates that fracture pressure is low, indicating a reopening of pre-existing fractures rather than fracturing of the intact formation. Observation of high-angle fractures within the massive reservoir sands in drillcore and field analogs (Ogata et al., 2012) supports a vertical to subvertical fracture model for the reservoir section. Fracture pressure can also generally be reduced due to the effect of poro-elasticity and/or cooling of the reservoir for the same reasons as for the horizontal stress on account of the observed low pore pressure (Fig. 12), and the possible larger difference between the temperature of the injection fluid and the formation temperature in the deeper, more permeable, reservoir units. A temperature difference between the injection water and the formation of up to 25°C might be expected based on temperature data (Elvebakk, 2010; Ogata et al., 2012).

Implications for the injection operation

For the Longyearbyen CO_2 pilot, the presence of pre-existing fractures combined with a very high tensile strength of intact rock implies that the most important factor controlling fracturing is the magnitude of in situ stresses. In order to ensure safe CO_2 storage, the reservoir pressure during the injection operation should be kept below the minimum principal stress in the cap rock at the top of the reservoir. The minimum principal stress

Table 3. *Summary of estimated vertical stress, interpreted minimum in situ stress, fracture pressure and tensile strength for the injection discussed in this study. The tensile strength σtv is normal to bedding plane, relevant for vertical fracturing, whereas σth is parallel with bedding and relevant for horizontal fracturing.*

Lithology/ Formation	Well No.	Testing interval (m)	Vertical stress* (bar)	Minimum In situ stress** (bar)	Fracture pressure† (bar)	Tensile strength‡ (bar)
Sandstone/ Helvetiafjellet	Dh6	171–181	40–47	-	42–43	σtv = 40–120 bar (Range of mechanical data for sandstone)
Shale/ Rurikfjellet	Dh6	300–309	69–81	63.5	83.5	σtv = 67 bar, σth = 40 bar (Mechanical data from fresh core, Dh6, same interval)
Shale/ Agardhfjellet	Dh6	420–435	96–113	94–104	115	σtv = 60 bar, σth = 30–50 bar (Mechanical data from well Dh2, 699 m, same formation)
Sandstone/ De Geerdalen	Dh7A	650–703	153–179	-	110–120	σtv = 40–120 bar (Range of data from mechanical data for sandstones)
Sandstone/ De Geerdalen	Dh4	870–970	207–244	-	130	σtv = 100–120 bar (Mechanical data, sandstones at deepest intervals)

*Vertical stress calculated for the middle of the testing interval for density range 2.3–2.7 g cm-3. **Based on the fracture closure pressure from LOT tests. †Based on LOT and SRT's. ‡Tensile strength is from mechanical testing (Table 1) and/or correlation log (Fig. 3).

in the overburden seems to be slightly lower but close to the vertical stress. We may then expect a reopening and flow along the existing network of natural fractures if the reservoir pressure exceeds these stress limits. Horizontal stress will represent the lower limit for the opening of vertical fractures, and vertical stress will represent the lower limit for the opening of horizontal fractures. The overall vertical migration of CO_2 will then depend on the connectivity between the natural fracture systems, where low-angle fractures (mainly in shales) will contribute to lateral fluid flow, while high-angle fractures (mainly in sandstones) will contribute to vertical fluid flow. Enhanced lateral connectivity might be expected at lithological boundaries, fracture set intersections and fracture corridors (e.g., in fault damage zones and chilled margins of intrusions) (Ogata et al., 2012).

Permeability of a fracture will be controlled by reopening and possible shearing of fractures in the reservoir due to CO_2 injection. A more detailed determination of shear deformation along fractures requires a more detailed assessment of fracture orientation and the in situ stress field, including the magnitude and orientation of the maximum horizontal stress (Chiaramonte et al., 2013; Lee et al., 2013). Shear deformation along fractures might enhance injectivity within the reservoir in the case of dilation and reduce injectivity in the case of mechanical destruction and breakdown of asperities during shearing (Barton & Choubey, 1977; Barton et al., 1985). Important parameters will be the shear strength of the fractured material and the actual effective normal and shear stresses acting on the fracture plane. In addition, total stress changes due to pore pressure build-up during storage and thermal effects also need to be considered.
Assuming a similar gradient of minimum horizontal stress and fracture pressure gradient throughout the overburden and down to the top reservoir, the minimum and vertical stress at the top of the reservoir (i.e., at 650 m depth) will be in the range of about 135 and 170 bar, respectively. The fracture pressure at the top of the reservoir is then assumed to be about 170 bar. The currently low reservoir pressure of 30–50 bar thus gives a significant pressure margin compared to these expected stresses and fracture pressures above the reservoir. However, there are significant uncertainties in both the in situ stresses and the fracture pressure that should be accounted for when establishing guidelines for the maximum allowable reservoir pressure and injection pressure for potential CO_2 injection operations (i.e., details in pore pressure and densities with depth). Note also that the values interpreted and reported in this paper are based on measurements for the locations of existing boreholes only, and that other regional factors might also have significant impacts on the magnitude of in situ stresses and borehole fracture pressures (i.e., topography around the injection site, the presence or absence of a permafrost layer in onshore vs. marine parts of the reservoir). These effects should also be accounted for when considering the integrity of the cap rock in lateral extensions during CO_2 plume migration.

Conclusions

Fracture pressure and in situ stresses for the overburden layers and the reservoir formations were obtained using geomechanical laboratory tests and injection tests in the wellbores. Combination of these two datasets enables us to assess the mechanical behaviour of the reservoir and cap rock during potential CO_2 storage operations. Laboratory tests showed that despite the shallow depth of the reservoir, less than 700 m, the strength and stiffness of the intact material are very high, and that there is a significant strength anisotropy in the shale units. The high tensile strength of intact formations in combination with the presence of pre-existing fractures makes it very unlikely that fracturing of the intact intervals will occur.
Interpretation of the injection tests shows that the fracture

pressure of the overburden is higher in magnitude and gradient than that in the reservoir. In the overburden, closure stress may represent a minor horizontal stress which is slightly lower than the vertical stress. Fracture pressure and pore pressure in the reservoir interval are significantly less than the vertical stress, which suggests that horizontal stress is the minimum principal stress. This suggests that reopening of vertical fractures is the most likely scenario for fracturing in the reservoir unit. For the overburden, the situation is more complex and the fracturing mode is uncertain due to the marginal difference between the minimum in situ stress and the vertical stress. Quite possibly the tensile strength of existing fractures (cohesion) and anisotropy in the shale might impact on the opening mode of the fractures in this overburden section.

Acknowledgements. The authors would like to thank SUCCESS for their financial support and the UNIS CO_2 Lab Pilot also for financial support, access to data and permission to publish. Two anonymous reviewers are thanked for constructive reviews of an earlier version of the paper.

References

ASTM 2010: D7012-07, Standard test method for compressive strength and elastic moduli of intact rock core specimens under varying states of stress and temperatures. Annual Book of ASTM Standards, ASTM International, West Conshohocken, PA, 1507 pp.

Bælum, K., Johansen, T., Johnsen, H., Roed, K., Ruud, B., Mikkelsen, E. & Braathen, A. 2012: Subsurface geometries of the Longyearbyen CO_2 lab in central Spitsbergen, as mapped by reflection seismic data. *Norwegian Journal of Geology 92*, 377–389.

Barton, N. & Choubey, V. 1977: The shear strength of rock joints in theory and practice. *Rock Mechanics 10*, 1–54.

Barton, N., Bandis, S. & Bakhtar, K. 1985: Strength, deformation and conductivity coupling of rock joints. International Journal of Rock *Mechanics and Mining Sciences & Geomechanics Abstracts 22*, 121–140.

Bergh, S.G., Braathen, A. & Andresen, A. 1997: Interaction of basement-involved and thin-skinned tectonism in the Tertiary fold-thrust belt of central Spitsbergen, Svalbard. *American Association of Petroleum Geologists Bulletin 81*, 637–661.

Biot, M. A. 1941: General theory of three dimensional consolidation. *Journal of Applied Physics 12*, 155–164.

Braathen, A., Bergh, S.G. & Maher, H.D. Jr. 1997: Thrust kinematics in the central part of the Tertiary transpressional fold-thrust belt in Spitsbergen. *Norges geologiske undersøkelse Bulletin 433*, 32–33.

Braathen, A., Bælum, K., Christiansen, H., Dahl, T., Flå, H., Hansen, F., Hanssen, T.H., Jochmann, M., Johansen, T.A., Mertes, J., Mørk, A., Nemec, W., Olaussen, S., Sand, G. & Tveranger, J. 2010: Longyearbyen CO_2 Lab 2007-2009 – Phase 1. Final Report. University Centre of Svalbard (UNIS) Report, 2010 – 2012, Longyearbyen, 69 pp.

Braathen, A., Balum, K., Christiansen, H., Dahl, T., Eiken, O., Elvebakk, H., Hansen, F., Hanssen, T., Jochmann, M. & Johansen, T. 2012: The Longyearbyen CO_2 Lab of Svalbard, Norway– initial assessment of the geological conditions for CO_2 sequestration. *Norwegian Journal of Geology 92*, 353–376.

Chiaramonte, L., White, J.A., Hao, Y. & Ringrose, P. 2013: Probabilistic Risk Assessment of Mechanical Deformation due to CO_2 Injection in a Compartmentalized Reservoir. *American Rock Mechanics Association, 47th US Rock Mechanics / Geomechanics Symposium, 23–26 June 2013, San Francisco, CA, USA*, 13–577.

Christiansen, H.H., Etzelmüller, B., Isaksen, K., Juliussen, H., Farbrot, H., Humlum, O., Johansson, M., Ingeman-Nielsen, T., Kristensen, L. & Hjort, J. 2010: The thermal state of permafrost in the Nordic area during the International Polar Year 2007–2009. *Permafrost and Periglacial Processes 21*, 156–181.

Elvebakk, H. 2010: Results of borehole logging in Well LYB CO_2, Dh4 of 2009, Longyearbyen, Svalbard. *NGU Report 2010.018*, 35 pp.

Gabrielsen, R. & Kløvjan, O. 1997: Late Jurassic—early Cretaceous caprocks of the southwestern Barents Sea: fracture systems and rock mechanical properties. *Norwegian Petroleum Society Special Publications 7*, 73–89.

Harrington, J.F., Noy, D.J., Horseman, S.T., Birchall, D.J. & Chadwick, R.A. 2009: Laboratory study of gas and water flow in the Nordland Shale, Sleipner, North Sea. *In* Grobe M., Pashin J.C., & Dodge R.L. (eds.): *Carbon dioxide sequestration in geological media – State of the science*. American Association of Petroleum Geologists Studies in Geology 59, pp. 521–543.

Hildenbrand, A., Schlömer, S. & Krooss, B. 2002: Gas breakthrough experiments on fine-grained sedimentary rocks. Geofluids 2, 3–23.

Horsrud, P. 2001: Estimating mechanical properties of shale from empirical correlations. *Society of Petroleum Engineers Drilling & Completion 16*, 68–73.

ISRM 2007: Suggested method for determining tensile strength of rock materials. *In* Ulusay, R. & Hudson, J.A. (eds.): *The complete ISRM suggested methods for rock characterization, testing and monitoring: 1974-2006*. International Society for Rock Mechanics, pp. 181–183.

Larsen, L. 2013: Analyses of DH4 Upper Zone Injection and Falloff Data, September 5 – October 15, 2013. 52 pp.

Lee, J., Min, K.-B. & Rutqvist, J. 2013: Probabilistic Analysis of Fracture Reactivation Associated with Deep Underground CO_2 Injection. *Rock Mechanics and Rock Engineering 46*, 801–820.

Lucier, A., Zoback, M., Gupta, N. & Ramakrishnan, T. 2006: Geomechanical aspects of CO_2 sequestration in a deep saline reservoir in the Ohio River Valley region. *Environmental Geosciences 13*, 85–103.

Magnabosco, C., Braathen, A. & Ogata, K. 2014: Permeability model of tight reservoir sandstones combining core-plug and Miniperm analysis of drillcore; Longyearbyen CO_2 Lab, Svalbard. *Norwegian Journal of Geology 94*, 189–200

Makurat, A., Torudbakken, B., Monsen, K. & Rawlings, C. 1992: Cenezoic uplift and caprock seal in the Barents Sea: fracture modelling and seal risk evaluation. *Society of Petroleum Engineers, SPE 24740*, 821–830.

Manum, S.B. & Throndsen, T.R. 1978: Rank of coal and dispersed organic matter and its geological bearing in the Spitsbergen Tertiary. *Norwegian Polar Institute yearbook 1977*, 159–177.

Mørk, M.B.E. 2013: Diagenesis and quartz cement distribution of low-permeability Upper Triassic–Middle Jurassic reservoir sandstones, Longyearbyen CO_2 lab well site in Svalbard, Norway. *American Association of Petroleum Geologists Bulletin 97*, 577–596.

NGI, 2010: Laboratory Testing – Janusfjellet cap rock material. NGI report 20061337–00–10–R, 22 pp.

Ogata, K., Senger, K., Braathen, A., Tveranger, J. & Olaussen, S. 2011: Natural Fractures in a Tight Reservoir for Potential CO_2 Storage (Spitsbergen, Svalbard)-Preliminary Results from Cores. *1st Sustainable Earth Sciences Conference & Exhibition (SES2011),8-11 November 2011, Valencia, Spain*.

Ogata, K., Senger, K., Braathen, A., Tveranger, J. & Olaussen, S. 2012: The importance of natural fractures in a tight reservoir for potential CO_2 storage: case study of the upper Triassic to middle Jurassic Kapp Toscana Group (Spitsbergen, Arctic Norway). *In* G.H. Spence, J. Redfern, R. Aguilera, T.G. Bevan, J.W. Cosgrove, G.D. Couples & J.-M. Daniel (eds.): *Advances in the Study of Fractured Reservoirs*, Geological Society of London Special Publication 374. Geological Society of London, doi:10.1144/SP374.9.

Raaen, A., Horsrud, P., Kjørholt, H. & Økland, D. 2006: Improved routine estimation of the minimum horizontal stress component from extended leak-off tests. *International Journal of Rock Mechanics and Mining Sciences 43,* 37–48.

Rutqvist, J., Birkholzer, J. & Tsang, C.-F. 2008: Coupled reservoir–geomechanical analysis of the potential for tensile and shear failure associated with CO_2 injection in multilayered reservoir–caprock systems. International *Journal of Rock Mechanics and Mining Sciences 45*, 132–143.

Senger, K., Planke, S., Polteau, S., Ogata, K. & Svensen, H. 2014: Sill emplacement and contact metamorphism of a siliclastic reservoir on Svalbard, Arctic Norway. *Norwegian Journal of Geology 94,* 155–169.

Skurtveit, E., Aker, E., Soldal, M., Angeli, M. & Wang, Z. 2012: Experimental investigation of CO_2 breakthrough and flow mechanisms in shale. *Petroleum Geoscience 18*, 3–15.

Terzaghi, K. 1943: *Theoretical soil mechanics*. John Wiley & Sons, New York,, 510 pp.

Throndsen, T. 1982: Vitrinite reflectance studies of coals and dispersed organic matter in tertiary deposits in the adventdalen area, Svalbard *Polar Research 1982*, 77–91.

Titlestad, G. O. 2010: Svalbard CO_2 Lab Post-job report, water injection test (Dh4), August 2010. *Gotic Report*, 87 pp.

Titlestad, G. O. 2011: Svalbard CO_2-lab Post-job report, Water injection tests-Dh6 September 2011. *Gotic Report*, 79 pp.

White, A.J., Traugott, M.O. & Swarbrick, R.E. 2002: The use of leak-off tests as means of predicting minimum in-situ stress. *Petroleum Geoscience 8*, 189–193.

Zhang, J. 2011: Pore pressure prediction from well logs: Methods, modifications, and new approaches. *Earth-Science Reviews 108*, 50–63.

Zoback, M.D. 2010: *Reservoir geomechanics*. Cambridge University Press, Cambridge, 449 pp.